



Katholieke Universiteit Leuven
Department of Mechanical Engineering
Celestijnenlaan 300B - bus 2420
B-3001 Heverlee (Belgium)

# Proceedings of **ISMA2008**

# International Conference on
# **Noise and Vibration Engineering**

## Volume I

September 15 to 17, 2008

Editors: Sas, P. and Bergen, B.

# Active porous composites for wide frequency-range noise absorption

**T. G. Zielinski**
Department of Intelligent Technologies
Institute of Fundamental Technological Research, Polish Academy of Sciences
ul.Swietokrzyska 21, 00-049, Warszawa, Poland
e-mail: **tzielins@ippt.gov.pl**

## Abstract

The paper presents a design, accurate multiphysics modeling and analysis of active porous-composite sound absorbers. Such absorbers are made up of a layer of poroelastic material (a porous foam) with embedded elastic implants having active (piezoelectric) elements. The purpose of such active composite material is to significantly absorb the energy of acoustic waves in a wide frequency range, particularly, in low frequencies. At the same time the total thickness of composites should be very moderate. The active parts of composites are used to adapt the absorbing properties of porous layers to different noise conditions by affecting the so-called solid-borne wave (originating mainly from the vibrations of elastic skeleton of porous medium) to counteract the fluid-borne wave (resulting mainly from the vibrations of air in the pores); the both waves are strongly coupled, especially, in lower frequencies. Passive and active performance of the absorbers is analysed to test the feasibility of this approach.

## 1 Introduction

There are apparent reasons for an advanced modeling of porous media with distributed masses and solid implants which should be at the same time sufficiently accurate and efficient to allow a reliable optimization of such poroelastic composites. Recent experimental investigations report a significant improvement of the insertion loss of standard acoustic blankets at lower frequencies by the addition of randomly placed masses to the poroelastic layers [1]. They show that the improvement by distributed masses (implants) tend to be greater than the one due to the mass effect alone. The acoustic absorption of multi-layer absorbers with different inner structures has also become a subject of research [2]. The proposed modeling was accurate with respect to the geometry (thanks to the finite element approach), however, the porous medium was modeled by using the so-called fluid-equivalent approach which generally assumes that the frame (solid skeleton) of a porous medium is rigid. For many porous materials such approach gives good predictions in higher frequencies and for certain configurations.

In the present paper the acoustic absorption of porous composites with active implants is examined. The absorption should be actively improved by affecting the vibrations of the elastic skeleton of porous layers. Thus, it is apparent that the rigid-frame approach cannot be used here. Instead, the advanced biphasic theory of poroelasticity is used to model porous material of the active absorbers.

First sections of this paper provide theoretical considerations and background concerning an accurate multiphysics modeling of the considered problem. Then, a few designs of porous composites are presented and results of the analyses of passive and active performance of these absorbers are discussed.

## 2 Multiphysics character of modeling

The examined application of active porous composites links several mathematical models of single- and multiphysics, namely:

- the Biot's theory poroelasticity – to model the material of porous layer (with the air-filled pores),
- the linear elasticity – to model elastic implants,
- the piezoelectricity – to model the active parts (piezo-actuators) of implants which affect the lower frequency vibrations of the elastic skeleton of a porous medium.

All these problems are strongly coupled and the consideration of this mutual interaction of different media is very important. Thus, a coupled multiphysics model of a system made up of poroelastic, elastic, and piezoelectric media (see Figure 1) was constructed using the Galerkin finite element method and the following weak integral:

$$\mathcal{WF}_{\mathrm{p}} + \mathcal{CI}_{\mathrm{p\text{-}e}} + \mathcal{WF}_{\mathrm{e}} + \mathcal{WF}_{\mathrm{pz}} = 0\,, \tag{1}$$

where $\mathcal{WF}_{\mathrm{p}}$, $\mathcal{WF}_{\mathrm{e}}$, $\mathcal{WF}_{\mathrm{pz}}$ are the weak forms of poroelasticity, elasticity, and piezoelectricity, respectively, whereas $\mathcal{CI}_{\mathrm{p\text{-}e}}$ is the coupling integral on the interface $\Gamma_{\mathrm{p\text{-}e}}$ between the poroelastic and elastic subdomains. The weak forms will be presented in the followings sections of this paper where it will be also shown that the coupling of the poroelastic and elastic media is naturally handled, i.e. $\mathcal{CI}_{\mathrm{p\text{-}e}} = 0$. Relevant boundary conditions will be discussed as well. The weak form of piezoelectricity $\mathcal{WF}_{\mathrm{pz}}$ can be substituted with the weak form of elasticity $\mathcal{WF}_{\mathrm{e}}$ by using a simplified approach based on some analogy with the thermoelasticity or, in other words, by introducing certain equivalent initial strains. As a matter of fact, this very approach can be used for the analyses presented in this paper. This approximation is justified here since the piezo-implants affect the vibrations of the less stiff skeleton of porous medium subjected to an acoustic wave excitation.

The considered vibroacoustic application allows for using linear theories, so the superposition principle holds and may be effectively used. Consequently, the frequency analysis may be used as an efficient tool for design and testing of the proposed active porous composites. Thus, all considered problems are time-harmonic with the frequency $f$ and the angular frequency $\omega = 2\pi f$.

The equations of poroelasticity presented below assume no body forces acting on the poroelastic material. Consequently, the problems of elasticity and piezoelectricity are considered with zero body forces. Moreover, in the piezoelectricity problem there is no body electric charge applied. These assumptions comply with the modeling requirements of the active porous composite noise absorbers.

For the sake of brevity, symbols $\mathrm{d}\Omega$ and $\mathrm{d}\Gamma$ are skipped in all the integrals presented below since it is obvious whether an integration is on the specified domain or boundary. The summation convention is used (for dummy indices $i, j, k, l$) and the (invariant) differentiation symbol which, in the Cartesian coordinate

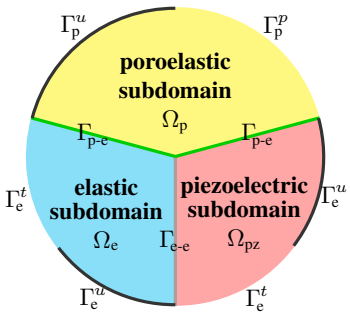


Figure 1: Multiphysics system made up of poroelastic, elastic, and piezoelectric media

system, simply reads: $(.)_{|i} = \frac{\partial(.)}{\partial x_i}$. The following notation rule applies for the symbol of variation (or test function): $\delta(v\,w) = v\,\delta w + w\,\delta v$, where $v$ and $w$ are two dependent variables (fields) and $\delta v$ and $\delta w$ their admissible variations.

# 3 Biot's theory of poroelasticity

## 3.1 The classical displacement formulation

The Biot's theory of poroelasticity [3, 4] provides a biphasic model of porous media: the so-called solid phase is used to describe the behavior of ('smeared') elastic skeleton whereas the fluid phase pertains to the fluid in the pores. The both phases are two coupled homogeneous continua. The most frequently used version of poroelasticity assumes besides that the both phases are isotropic. Moreover, the fluid is modelled as inviscid, though viscous forces, are taken into account but only when modeling interaction between the fluid and the solid frame.

In the classical formulation [3, 4] a state of poroelastic medium is described by the displacements of solid, $\boldsymbol{u} = \{u_i\}$, and fluid phase, $\boldsymbol{U} = \{U_i\}$. The Biot's equations for a local dynamic equilibrium of poroelastic material link partial stress tensors associated with the skeleton particle ($\sigma^{\mathrm{s}}_{ij}$) and the macroscopic fluid particle ($\sigma^{\mathrm{f}}_{ij}$) with the solid and fluid macroscopic displacements. In the case of harmonic oscillations (with angular frequency $\omega$) these equations read

$$\sigma^{\mathrm{s}}_{ij|j} + \omega^2\,\tilde{\varrho}_{\mathrm{ss}}\,u_i + \omega^2\,\tilde{\varrho}_{\mathrm{sf}}\,U_i = 0\,, \qquad \sigma^{\mathrm{f}}_{ij|j} + \omega^2\,\tilde{\varrho}_{\mathrm{ff}}\,U_i + \omega^2\,\tilde{\varrho}_{\mathrm{sf}}\,u_i = 0\,, \tag{2}$$

where the frequency-dependent effective densities, $\tilde{\varrho}_{\mathrm{ss}}$, $\tilde{\varrho}_{\mathrm{sf}}$, and $\tilde{\varrho}_{\mathrm{ff}}$, are introduced. These densities are responsible not only for the inertia of solid or fluid phase particles but also for the combined inertial and viscous coupling (interaction) of both phases. They depend on the viscous drag coefficient, $\tilde{b}$, and the normal effective densities, $\varrho_{\mathrm{ss}}$, $\varrho_{\mathrm{ff}}$, $\varrho_{\mathrm{sf}}$. The latter quantities in turn depend on the porosity, $\phi$, the tortuosity of pores, $\alpha_\infty$, the density of the material of skeleton, $\varrho_{\mathrm{s}}$, and the density of saturating fluid, $\varrho_{\mathrm{f}}$. The adequate formulas may be found in [4].

The partial solid and fluid stress tensors are linearly related to the partial strain tensors prevailing in the skeleton and the interstitial fluid. This is given by the following linear and isotropic constitutive equations of the Biot's theory of poroelasticity:

$$\sigma^{\mathrm{s}}_{ij} = \mu_{\mathrm{s}}\,(u_{i|j} + u_{j|i}) + \Big(\tilde{\lambda}_{\mathrm{s}}\,u_{k|k} + \tilde{\lambda}_{\mathrm{sf}}\,U_{k|k}\Big)\delta_{ij}\,, \quad \sigma^{\mathrm{f}}_{ij} = \Big(\tilde{\lambda}_{\mathrm{f}}\,U_{k|k} + \tilde{\lambda}_{\mathrm{sf}}\,u_{k|k}\Big)\delta_{ij}\,. \tag{3}$$

Four material constants are involved here, namely $\mu_{\mathrm{s}}$, $\tilde{\lambda}_{\mathrm{s}}$, $\tilde{\lambda}_{\mathrm{f}}$, and $\tilde{\lambda}_{\mathrm{sf}}$. The first two of them resemble the two Lamé coefficients of isotropic elasticity. Moreover, $\mu_{\mathrm{s}}$ is the shear modulus of the poroelastic material and consequently the shear modulus of the frame since the fluid does not contribute to the shear restoring force. The three dilatational constants, $\tilde{\lambda}_{\mathrm{s}}$, $\tilde{\lambda}_{\mathrm{f}}$ and $\tilde{\lambda}_{\mathrm{sf}}$ are frequency-dependent and are functions of $K_{\mathrm{b}}$, $K_{\mathrm{s}}$, and $\tilde{K}_{\mathrm{f}}$ ($\tilde{\lambda}_{\mathrm{s}}$ depends also on $\mu_{\mathrm{s}}$), where: $K_{\mathrm{b}}$ is the bulk modulus of the frame at constant pressure in the fluid, $K_{\mathrm{s}}$ is the bulk modulus of the elastic solid from which the frame is made, and $\tilde{K}_{\mathrm{f}}$ is the bulk modulus of the fluid. The adequate formulas to compute the poroelastic material constants can be found in [4]. Finally, the total stress tensor of poroelastic medium is defined as a simple sum of the partial, i.e. phasic, stress tensors, whereas the total displacement vector sums up porosity-dependent contributions of the displacements of both phases:

$$\sigma^{\mathrm{t}}_{ij} = \sigma^{\mathrm{s}}_{ij} + \sigma^{\mathrm{f}}_{ij}\,, \qquad u^{\mathrm{t}}_i = (1-\phi)\,u_i + \phi\,U_i\,. \tag{4}$$

The equations of equilibrium (2) together with the constitutive relations (3) form the displacement formulation of linear, isotropic poroelasticity for harmonic oscillations. Notice that the first equations from the both pairs refer to the solid phase whereas the second ones to the fluid phase. Nevertheless, the both phases are strongly coupled by the viscous-inertial coupling coefficient, $\tilde{\varrho}_{\mathrm{sf}}$, and the constitutive coupling constant, $\tilde{\lambda}_{\mathrm{sf}}$. In this classical formulation the unknown fields are the solid and fluid phase displacements, which means 6 degrees of freedom in every node of a three-dimensional model.

### 3.2 The mixed displacement–pressure formulation

The fluid phase stress tensor can be expressed as

$$\sigma_{ij}^{\mathrm{f}} = -\phi\, p\, \delta_{ij}\,, \tag{5}$$

where $p$ is the pressure of fluid in the pores (it should not be mistaken for the pressure of fluid phase which equals $\phi p$). By using this relation for the time-harmonic veriosn of the Biot's poroelasticity, the fluid phase displacements can be expressed as functions of the pressure in the pores, and thus eliminated from the equations (replaced by $p$). This results in the mixed displacement–pressure formulation [5, 6] where the dependent variables are the three solid phase displacements and the pore-fluid pressure. Therefore, three-dimensional models have now only 4 degrees of freedom in a node.

### 3.3 Weak integral form of the mixed formulation of poroelasticity

Let $\Omega_{\mathrm{p}}$ be a domain of poroelastic material and $\Gamma_{\mathrm{p}}$ its boundary with $n_i$ being the components of the unit vector normal to the boundary and pointing outside the domain. The harmonic poroelasticity problem can be described in this domain by the mixed formulation which uses as dependent variables the solid phase displacements, $u_i$, and pore-fluid pressure, $p$. The corresponding weak form [7] reads as follows (for every admissible $\delta u_i$ and $\delta p$)

$$\begin{aligned}\mathcal{WF}_{\mathrm{p}} = &-\int_{\Omega_{\mathrm{p}}} \sigma_{ij}^{\mathrm{ss}}\, \delta u_{i|j} + \int_{\Omega_{\mathrm{p}}} \omega^2\, \tilde{\varrho}\, u_i\, \delta u_i - \int_{\Omega_{\mathrm{p}}} \frac{\phi^2}{\omega^2\, \tilde{\varrho}_{\mathrm{ff}}}\, p_{|i}\, \delta p_{|i} + \int_{\Omega_{\mathrm{p}}} \frac{\phi^2}{\tilde{\lambda}_{\mathrm{f}}}\, p\, \delta p \\ &+ \int_{\Omega_{\mathrm{p}}} \phi \left(1 + \frac{\tilde{\varrho}_{\mathrm{sf}}}{\tilde{\varrho}_{\mathrm{ff}}}\right) \delta(p_{|i}\, u_i) + \int_{\Omega_{\mathrm{p}}} \phi \left(1 + \frac{\tilde{\lambda}_{\mathrm{sf}}}{\tilde{\lambda}_{\mathrm{f}}}\right) \delta(p\, u_{i|i}) + \mathcal{BI}_{\mathrm{p}} = 0\,,\end{aligned} \tag{6}$$

where

$$\sigma_{ij}^{\mathrm{ss}} = \mu_{\mathrm{s}}\, (u_{i|j} + u_{j|i}) + \left(\tilde{\lambda}_{\mathrm{s}} - \frac{\tilde{\lambda}_{\mathrm{sf}}^2}{\tilde{\lambda}_{\mathrm{f}}}\right) u_{k|k}\, \delta_{ij} \quad \text{and} \quad \tilde{\varrho} = \tilde{\varrho}_{\mathrm{ss}} - \frac{\tilde{\varrho}_{\mathrm{sf}}^2}{\tilde{\varrho}_{\mathrm{ff}}}\,, \tag{7}$$

$\mathcal{BI}_{\mathrm{p}}$ is the boundary integral

$$\mathcal{BI}_{\mathrm{p}} = \int_{\Gamma_{\mathrm{p}}} \sigma_{ij}^{\mathrm{t}}\, n_j\, \delta u_i + \int_{\Gamma_{\mathrm{p}}} \phi\, (U_i - u_i)\, n_i\, \delta p\,, \tag{8}$$

whereas $\delta u_i$ and $\delta p$ are test (or weighting) functions, that is, arbitrary yet admissible virtual displacements and pressure. Below, the two most relevant boundary conditions of poroelastic medium are discussed [6, 7].

### 3.4 Relevant boundary conditions for poroelastic medium

#### 3.4.1 Imposed displacement field

A displacement field, $\hat{u}_i$, applied on a boundary of a poroelastic medium describes, for example, a case of a piston in motion acting on the surface of the medium. Here, it is assumed that the solid skeleton is fixed to the surface of piston while the fluid obviously cannot penetrate into the piston. Therefore, on $\Gamma_{\mathrm{p}}^u$:

$$u_i = \hat{u}_i\,, \qquad (U_i - u_i)\, n_i = 0\,. \tag{9}$$

The first condition expresses the continuity between the imposed displacement vector and the solid phase displacement vector. The second equation expresses the continuity of the normal displacements between the solid phase and the fluid phase. Using these conditions and the fact that the variations of the known solid displacements are zero ($\delta u_i = 0$) the boundary integral reduces to zero (on the relevant part of the boundary):

$$\mathcal{BI}_{\mathrm{p}} = 0 \text{ on } \Gamma_{\mathrm{p}}^u\,. \tag{10}$$

### 3.4.2 Imposed pressure field

A harmonic pressure field of amplitude $\hat{p}$ is imposed on the boundary of a poroelastic domain which means that it affects at the same time the fluid in the pores and the solid skeleton. Therefore, the following boundary conditions must be met on $\Gamma_{\mathrm{p}}^{p}$:

$$p = \hat{p}\,, \qquad \sigma_{ij}^{\mathrm{t}}\, n_j = -\hat{p}\, n_i\,. \tag{11}$$

The first condition is of Dirichlet type and must be applied explicitly. It describes the continuity of pressure in the fluid. It means also that the pressure variation is zero ($\delta p = 0$) at the boundary. The second condition expresses the continuity of the total normal stress. All this, when used for Equation (8), leads to the following boundary integral

$$\mathcal{BL}_{\mathrm{p}} = \int\limits_{\Gamma_{\mathrm{p}}} \sigma_{ij}^{\mathrm{t}}\, n_j\, \delta u_i = -\int\limits_{\Gamma_{\mathrm{p}}^{p}} \hat{p}\, n_i\, \delta u_i\,. \tag{12}$$

# 4 Weak form of elasticity, an approximation of piezoelectricity, and coupling to poroelastic media

## 4.1 Weak form for an elastic solid

Let $\Omega_{\mathrm{e}}$ be an elastic solid domain with mass density $\varrho_{\mathrm{e}}$ and boundary $\Gamma_{\mathrm{e}}$, and $n_i^{\mathrm{e}}$ the components of unit vector normal to the boundary and pointing outside the domain. Assuming zero body forces and the case of harmonic oscillations the weak variational form of the problem of elasticity expressing the principle of virtual work reads (for every admissible $\delta u_i^{\mathrm{e}}$)

$$\mathcal{WF}_{\mathrm{e}} = -\int\limits_{\Omega_{\mathrm{e}}} \sigma_{ij}^{\mathrm{e}}\, \delta u_{i|j}^{\mathrm{e}} + \int\limits_{\Omega_{\mathrm{e}}} \omega^2 \varrho_{\mathrm{e}}\, u_i^{\mathrm{e}}\, \delta u_i^{\mathrm{e}} + \int\limits_{\Gamma_{\mathrm{e}}} \sigma_{ij}^{\mathrm{e}}\, n_j^{\mathrm{e}}\, \delta u_i^{\mathrm{e}} = 0\,, \tag{13}$$

where $\delta u_i^{\mathrm{e}}$ is the arbitral yet admissible variation of displacements; the elastic stress tensor $\sigma_{ij}^{\mathrm{e}} = \sigma_{ij}^{\mathrm{e}}(\boldsymbol{u}^{\mathrm{e}})$ substitutes here a linear function of elastic displacements $\boldsymbol{u}^{\mathrm{e}} = \{u_i^{\mathrm{e}}\}$. In the case of the linear isotropic elasticity it can be expressed as follows

$$\sigma_{ij}^{\mathrm{e}} = \mu_{\mathrm{e}}\,(u_{i|j}^{\mathrm{e}} + u_{j|i}^{\mathrm{e}}) + \lambda_{\mathrm{e}}\, u_{k|k}^{\mathrm{e}}\, \delta_{ij}\,, \tag{14}$$

where the well-known Lamé coefficients, the shear modulus $\mu_{\mathrm{e}}$ and the dilatational constant $\lambda_{\mathrm{e}}$, appear. Before discussing the corresponding boundary conditions for an elastic solid, a thermoelastic analogy approach to the approximation of piezoelectricity will be presented.

## 4.2 Approximation of piezoelectricity by initial strains

As mentioned above, a piezoelectric domain can be often modeled as an elastic medium with some initial strain or, equivalently, subject to a specific thermal load. This approximation is based on the resemblance between the thermoelastic and converse-piezoelectric constitutive equations: the stress vs. strain and voltage equation of piezoelectricity resembles the Hooke's law with initial strains (induced, for example, by a temperature field). The initial strain simulates the piezoelectric effect. Thus, in this approach the weak form of elasticity (13) is used for a piezoelectric domain $\Omega_{\mathrm{pz}}$ with

$$\sigma_{ij}^{\mathrm{e}} = C_{ijkl}^{\mathrm{pz}}\big(\varepsilon_{kl}^{\mathrm{e}} - \varepsilon_{kl}^{0}\big)\,, \tag{15}$$

where $\varepsilon_{kl}^{\mathrm{e}} = \frac{u_{k|l}^{\mathrm{e}} + u_{k|l}^{\mathrm{e}}}{2}$ are simple elastic strains, and

$$\varepsilon_{kl}^{0} = d_{ikl}^{\mathrm{pz}}\, E_i^{\mathrm{pz}} = -d_{ikl}^{\mathrm{pz}}\, V_{|i}^{\mathrm{pz}} \tag{16}$$

are the initial elastic strains approximating the piezoelectric effect. Furthermore, $C^{\text{pz}}_{ijkl}$ and $d^{\text{pz}}_{ikl}$ denote the components of the fourth-order (orthotropic or transversally isotropic) tensor of elastic material constants and the third-order tensor of piezoelectric material constants, respectively, whereas $E^{\text{pz}}_i$ and $V^{\text{pz}}$ are the electric field and electric potential; they are related by the Maxwell's law for electricity:

$$E^{\text{pz}}_i = -V^{\text{pz}}_{|i} \,. \tag{17}$$

In this approximation the electric problem is uncoupled from its mechanical counterpart and can be solved independently. Thus, the electric potential $V^{\text{pz}}$ is found by solving the following equation of electricity (presented here with no body electric charge) in the piezoelectric domain $\Omega_{\text{pz}}$:

$$\epsilon^{\text{pz}}_{ji}\, V^{\text{pz}}_{|ij} = 0 \,, \tag{18}$$

where $\epsilon^{\text{pz}}_{ji}$ denote the tensor of dielectric material constants, with the following electrical boundary conditions (of the Neumann and Dirichlet kind, respectively):

$$\epsilon^{\text{pz}}_{ji}\, V^{\text{pz}}_{|i}\, n^{\text{pz}}_j = \hat{Q}^{\text{pz}} \text{ on } \Gamma^{Q}_{\text{pz}} \,, \qquad V^{\text{pz}} = \hat{V}^{\text{pz}} \text{ on } \Gamma^{V}_{\text{pz}} \,. \tag{19}$$

The Neumann condition serves for a surface electric charge $\hat{Q}^{\text{pz}}$ applied on a boundary, whereas the Dirichlet condition allows to prescribe the electric potential $\hat{V}^{\text{pz}}$ on a boundary. Now, the electric vector field can be computed from the Maxwell's law (17), and the 'piezo-equivalent' initial strain can be found from Equation (16). In practice, for thin piezoelectric patches with electrodes on the opposite sides so that the electric voltage $\Delta\hat{V}^{\text{pz}}$ is applied across the $x_3$-direction the electric potential field can be determined as follows: $E^{\text{pz}}_3 = \frac{\Delta\hat{V}^{\text{pz}}}{\text{thickness}}$ and $E^{\text{pz}}_1 = E^{\text{pz}}_2 = 0$.

## 4.3 Elastic solid boundary conditions

For the sake of brevity, only von Neumann and Dirichlet boundary conditions for an elastic solid will be discussed here (the Robin type involves the technique of Lagrange multipliers and will be skipped). The Neumann (or natural) boundary conditions describe the case when forces $\hat{t}^{\text{e}}_i$ are applied on a boundary, that is

$$\sigma^{\text{e}}_{ij}\, n^{\text{e}}_j = \hat{t}^{\text{e}}_i \text{ on } \Gamma^{t}_{\text{e}} \,, \tag{20}$$

whereas the displacements, $\hat{u}^{\text{e}}_i$, are prescribed by the Dirichlet (or essential) boundary conditions

$$u^{\text{e}}_i = \hat{u}^{\text{e}}_i \text{ on } \Gamma^{u}_{\text{e}} \,. \tag{21}$$

According to these conditions the boundary is divided into two (directionally disjoint) parts, i.e. $\Gamma_{\text{e}} = \Gamma^{t}_{\text{e}} \cup \Gamma^{u}_{\text{e}}$. There is an essential difference between the two kinds of conditions. The displacement constraints form the kinematic requirements for the trial functions, $u^{\text{e}}_i$, while the imposed forces appear in the weak form; thus, the boundary integral, that is the last of the integrals of Equation (13), equals

$$\mathcal{BI}_{\text{e}} = \int_{\Gamma_{\text{e}}} \sigma^{\text{e}}_{ij}\, n^{\text{e}}_j\, \delta u^{\text{e}}_i = \int_{\Gamma^{t}_{\text{e}}} \hat{t}^{\text{e}}_i\, \delta u^{\text{e}}_i \,. \tag{22}$$

Here, the property $\delta u^{\text{e}}_i = 0$ on $\Gamma^{u}_{\text{e}}$ has been used.

## 4.4 Poroelastic–elastic coupling

Let $\Gamma_{\text{p-e}}$ be the interface between poroelastic and elastic media. Let $n_i$ be the components of the unit vector normal to the interface and pointing outside the poroelastic domain into the elastic one. The coupling integral

combines boundary integral terms resulting from both, poroelastic and elastic, weak forms (Equations (6)-(8) and (13)-(14) or (15), respectively):

$$\mathcal{CI}_{\text{p-e}} = \int_{\Gamma_{\text{p-e}}} \sigma^{\text{t}}_{ij}\, n_j\, \delta u_i + \int_{\Gamma_{\text{p-e}}} \phi\, (U_i - u_i)\, n_i\, \delta p + \int_{\Gamma_{\text{p-e}}} \sigma^{\text{e}}_{ij}\, n^{\text{e}}_j\, \delta u^{\text{e}}_i \tag{23}$$

where $n^{\text{e}}_i = -n_i$ are the components of the unit normal vector pointing outside the elastic domain (and into the poroelastic medium). Now, the following coupling conditions must be met at the interface $\Gamma_{\text{p-e}}$:

$$\sigma^{\text{t}}_{ij}\, n_j = \sigma^{\text{e}}_{ij}\, n_j\,, \qquad (U_i - u_i)\, n_i = 0\,, \qquad u_i = u^{\text{e}}_i\,, \tag{24}$$

The first condition states the continuity of total stress tensor, the second expresses that there is no mass flux across the interface, and the last one assumes the continuity of the solid displacements [7]. This last condition means also the equality of the variations of displacements, $\delta u_i = \delta u^{\text{e}}_i$. Now, applying the coupling conditions for the coupling integral (23) results in

$$\mathcal{CI}_{\text{p-e}} = 0\,. \tag{25}$$

# 5 Acoustic absorption of a poroelastic layer

The main purpose of the present analysis of poroelastic layers with solid implants is to asses how the passive and active implants can influence the acoustic absorption of layers. The acoustic absorption of a poroelastic layer fixed to a rigid wall and subject to a plane acoustic wave propagating in the air onto the layer surface at normal incidence will be computed as follows [4]. First, the acoustic impedance at normal incidence is determined at the interface between the poroelastic layer and the air:

$$Z = \frac{p_0}{v}\,, \quad \text{where} \quad v = \mathrm{j}\,\omega\, u^{\text{t}}_1 = \mathrm{j}\,\omega\, \left[(1-\phi)\, u_1 + \phi\, U_1\right]. \tag{26}$$

Here, $v$ is the velocity of propagating wave at the layer–air interface (continuous across this boundary) whereas $p_0$ is the wave pressure. As a matter of fact the (complex) amplitudes are used here. Now, the reflection coefficient in this point is computed:

$$R = \frac{Z - Z_0}{Z + Z_0}\,, \tag{27}$$

where $Z_0 = \varrho_0\, c_0$ is the characteristic impedance of the air ($\varrho_0$ is the air density and $c_0$ the speed of sound). Finally, knowing the reflection coefficient, the acoustic absorption coefficient can be determined:

$$A = 1 - |R|^2\,. \tag{28}$$

This final property is real-valued (unlike the reflection coefficient $R$, and the impedance $Z$, which are complex).

# 6 Results and discussion of finite-element analyses

## 6.1 Analyzed configurations

Several finite element analyses of poroelastic layers with (or without) solid implants were carried out for configurations presented in Figure 2. The configurations are two-dimensional (in the $x_1x_2$-plane) so the adequate extrusion in the $x_3$-direction is assumed. Nevertheless, this approach should also give good predictions for similar three-dimensional configurations of sufficient regularity.

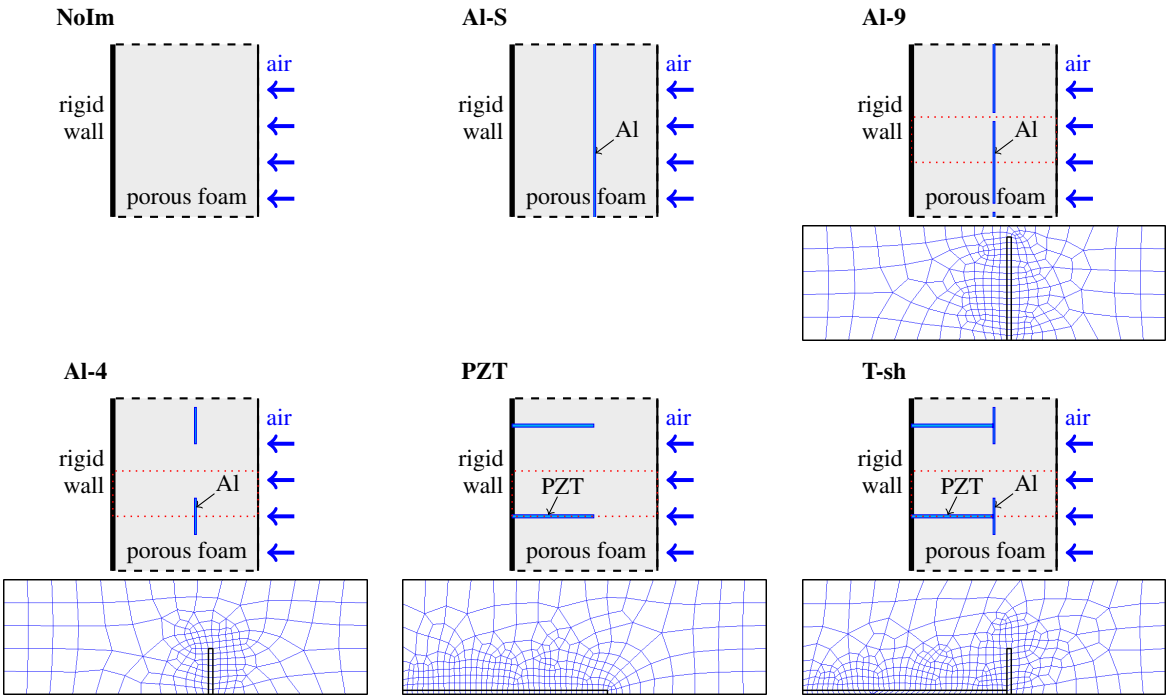


Figure 2: Analyzed configurations of porous composites and the corresponding finite-element meshes of the representative subdomain. The total thickness of each composite is 16 mm (see also Figure 3 for other dimensions). The configurations are layers of poroelastic foam and differ only by the embedded implants, as follows: **NoIm** – no implants, **Al-S** – a septum of aluminium foil, **Al-9** – 9 mm-wide stripes of aluminium foil, **Al-4** – 4 mm-wide stripes of aluminium foil, **PZT** – fixed PZT-implants, **T-sh** – active T-shaped implants.

| | | Foam A | Foam B |
|---|---|---|---|
| porosity | $\phi$ | 0.97 | 0.99 |
| tortuosity | $\alpha_\infty$ | 2.52 | 1.98 |
| flow resistivity | $\sigma$ | $87\,\mathrm{kN\,s/m^4}$ | $65\,\mathrm{kN\,s/m^4}$ |
| characteristic dimension of pores: | | | |
| – for viscous forces | $\Lambda$ | $37\cdot10^{-6}\mathrm{m}$ | $37\cdot10^{-6}\mathrm{m}$ |
| – for thermal forces | $\Lambda'$ | $119\cdot10^{-6}\mathrm{m}$ | $121\cdot10^{-6}\mathrm{m}$ |
| solid-phase mass density | $\varrho_{\mathrm{sph}}$ | $31\,\mathrm{kg/m^3}$ | $16\,\mathrm{kg/m^3}$ |
| shear modulus | $\mu_{\mathrm{s}}$ | $55(1+\vartheta\mathrm{j})$ kPa | $18(1+\vartheta\mathrm{j})$ kPa |
| loss factor | $\vartheta$ | 0.055 | 0.1 |
| bulk Poisson's ratio | $\nu_{\mathrm{b}}$ | 0.3 | 0.3 |

Table 1: Poroelastic properties of two polyurethane foams

Poroelastic material data for two different high-porosity polyurethane foams (termed A and B) was used for the configurations. This data is given in Table 1 and for the Biot's model of poroelastic medium it should be supplemented with the density, bulk modulus, viscosity, ratio of specific heats, ambient mean pressure, and the Prandtl number for the air.

The total thickness of layer in each configuration is always 16 mm. At $x_1 = 0$ mm the layer is fixed to a rigid wall whereas at $x_1 = 16$ mm the plane harmonic acoustic wave propagates onto the interface between the poroelastic layer and the air. The following six configurations were analyzed (see Figure 2):

**NoIm** – a simple "homogeneous" layer of porous foam with **no implants**;

**Al-S** – two layers of porous foam linked by a **septum** of 0.3 mm-thick **aluminium** foil;

**Al-9** – a layer of porous foam with densely-set **9 mm**-wide stripes of 0.3 mm-thick **aluminium** foil;

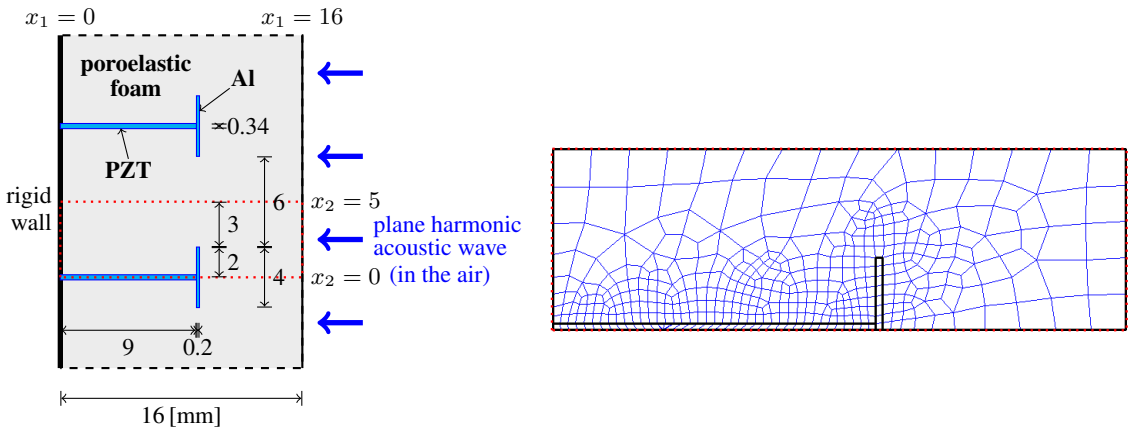


Figure 3: Active composite configuration and the finite-element mesh of the modeled representative subdomain

**Al-4** – a layer of porous foam with loosely-set **4 mm**-wide stripes of 0.3 mm-thick **aluminium** foil;

**PZT** – a layer of porous foam with parallel **PZT**-implants fixed to a rigid wall;

**T-sh** – a layer of porous foam with **T-shaped** implants made up of stripes of 0.3 mm-thick aluminium foil fixed to the the active PZT-elements.

The first four configurations are passive, while the configurations **PZT** and **T-sh** have active elements. The results of the acoustic absorption in passive and active states will be presented for the last configuration with T-shaped implants (see Figure 3). Notice that this configuration is, in fact, a combination of the configurations **Al-4** and **PZT**.

As mentioned above, the problem is modelled as two-dimensional, in the $x_1x_2$-plane. Moreover, the symmetry (regularity along the $x_2$-axis) makes it possible to model only a rectangular slice (of width $\Delta x_2 = 5$ mm) of the layer comprising only a half of one implant (see Figures 2 and 3) by applying proper boundary conditions. For some configurations the corresponding finite-element meshes are given. Such meshes are not presented for the configurations **NoIm** and **Al-S** since for such regular (multi)layered media planar analytical solutions can be used (in fact, the finite-element analyses were also performed for these two cases and gave the identical results with the corresponding 1-dimensional analytical solutions). All necessary dimensions for the active composite **T-sh** are given in Figure 3, where the finite-element mesh of the representative modeled subdomain is also shown. Relevant dimensions from this figure are also valid for other configurations.

The analysis consisted in determining the acoustic absorption of the poroelastic composites. To this end, the results of finite-element analysis (especially, $u_1^{\mathrm{t}}$ at the layer's surface) were used by the analytical formulas for the impedance, the reflection and absorption coefficients (see Section 5). These formulas result from a one-dimensional analysis of the plane wave propagation which is slightly violated if the solid implants are present (notice, however, that the implants are set approximately 7 mm form the surface of the free-interface). Therefore, the absorption coefficient was computed in two points of the layer surface: at $x_2 = 0$ mm and $x_2 = 5$ mm (see Figure 3), providing two limit-values. It was checked that in the considered frequency range the two values are almost always very similar and thus, for the sake of clearness, only the average curve is plotted in the graphs presented below.

## 6.2 Acoustic absorption of the passive poroelastic composites

Figure 4 presents the acoustic absorption of passive poroelastic composites compared to the absorption of the porous layer without implants; the porous material was foam A with properties presented in Table 1. The upper graph shows the absorption curves for the layer with a continuous septum made up of 0.2 mm-thick

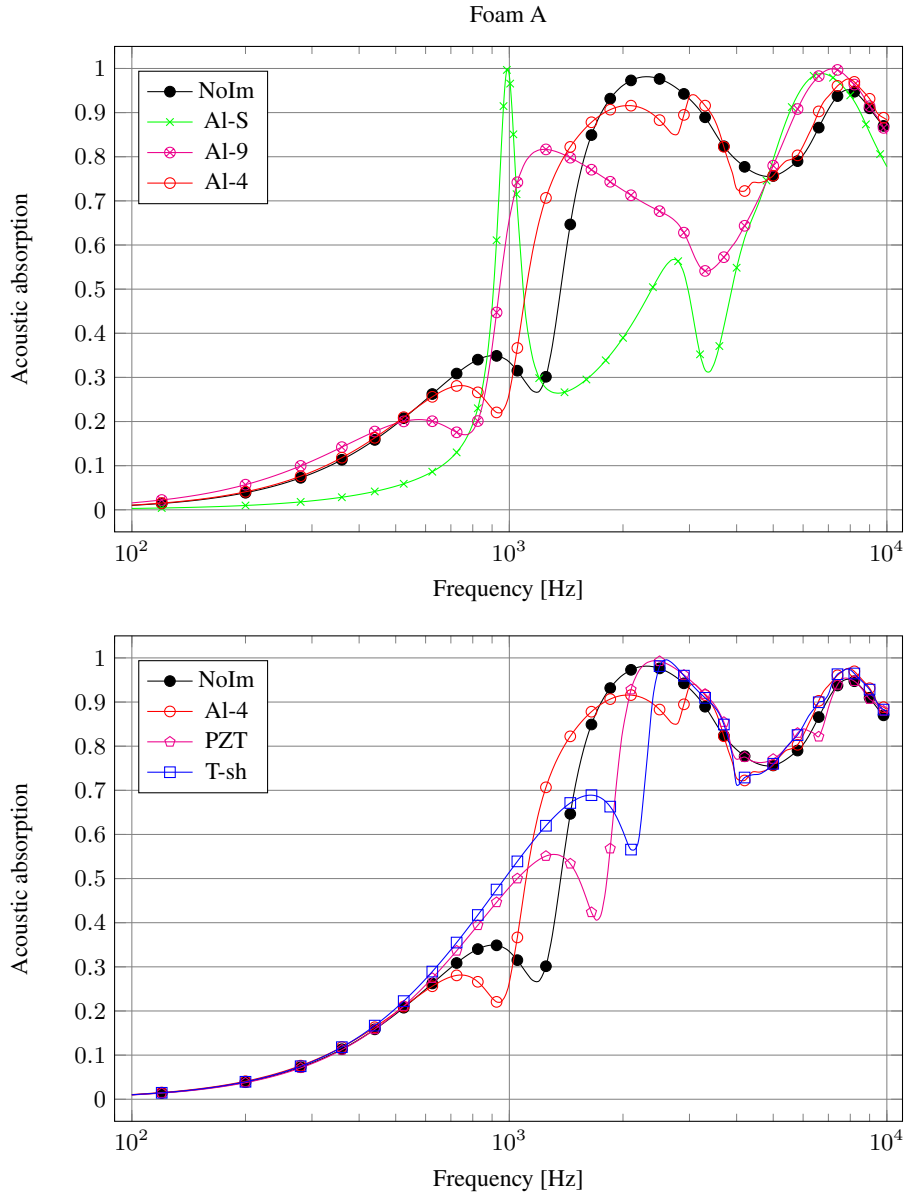


Figure 4: Passive absorption curves for the porous composite/layer made of the foam A

aluminium foil, and for the layers with aluminium stripes (9 mm or 4 mm wide) made up of the same foil. The composite with the continuous septum deteriorates generally the acoustic absorption although it exhibits a great performance around a particular single frequency (i.e. 1000 Hz). The composites with the aluminium stripes improve the absorption in some frequency range but deteriorate it in another. The lower graph of Figure 4 shows the acoustic absorption of the layer with no implants compared with the absorption curves of three composites: with 4 mm-wide aluminium stripes,with fixed (passive) PZT implants, and with complete (passive) T-shaped implants. For the lowest frequencies (up to 600 Hz) there is no difference between the curves: the absorption is poor since nothing can be done with layers only 16 mm thick. Between 600 to 3000 Hz the absorption of composites with implants is better in some range of frequencies and worse in another range. Above 2100 Hz (for PZT), 2500 Hz (for T-sh), or 3000 Hz (for Al-4) the absorption curves of composites are similar to the absorption curve of "homogeneous" layer.

Similar analysis was performed for the layer and composites made up of foam B (see Table 1 for its poroelastic properties). The results of the acoustic absorption are presented in Figure 5 and since the thickness of layers, inner geometry and material of implants are the same as for the composites made up of the foam A,

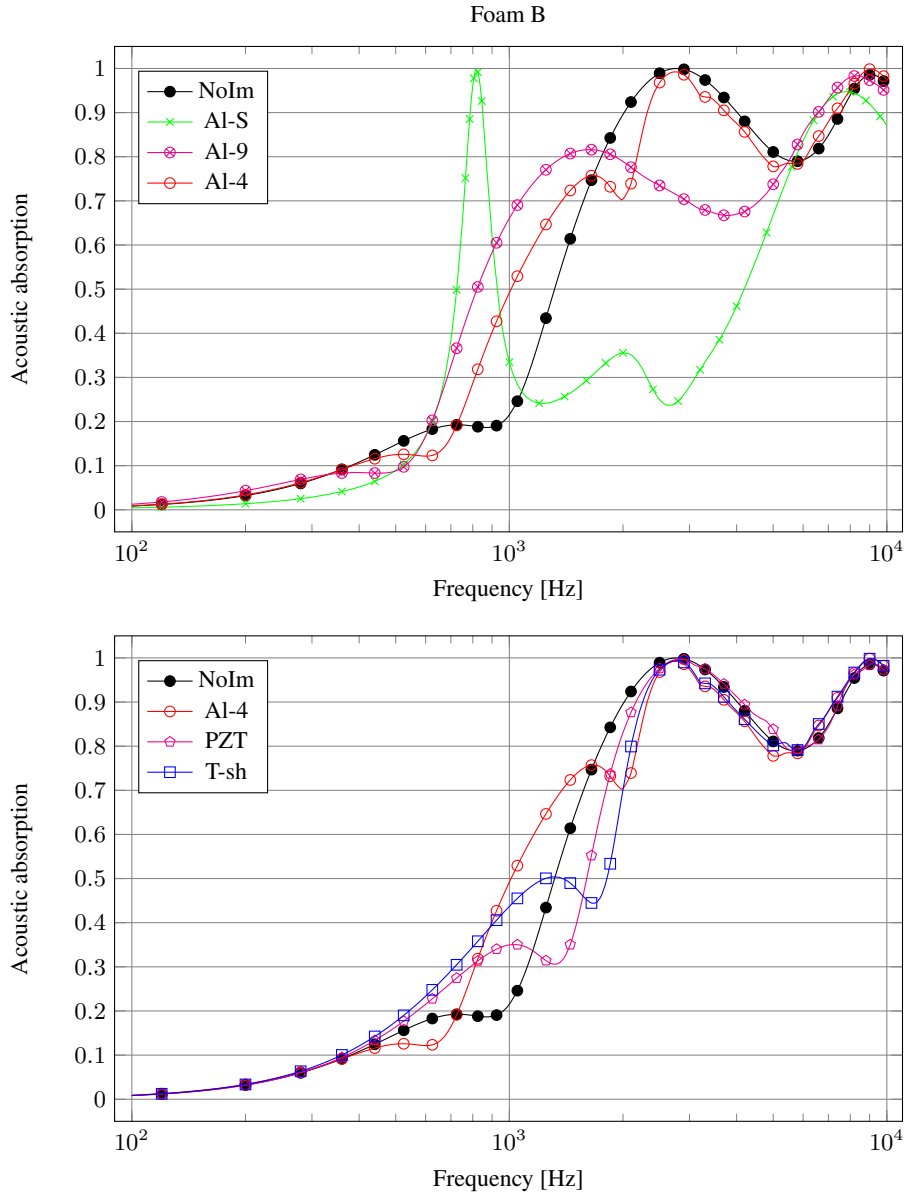


Figure 5: Passive absorption curves for the porous composite/layer made of the foam B

the conclusions are also similar. The composite Al-S (with the continuous aluminium septum) has the worst absorption with the exception of a narrow range around 800 Hz where locally the absorption approaches 1. The composite Al-9 has the best absorption between 700 and 1800 Hz but worse for other frequencies. There is no significant difference in the absorption curves of "homogeneous" layer and the porous composites Al-4, PZT, and T-sh for frequencies lower than 500 Hz or higher than 2700 Hz. In between, the composites have better performance in some range of frequencies and worse in another range.

The general conclusion is that the T-shaped implants change the absorption in a range of medium frequencies: they improve it for the lower-frequency part of this range (where the absorption is weak) and deteriorate it at higher frequencies (where the absorption is better altogether). Still, an active approach should be tried to get the best performance in the widest frequency range.

## 6.3 Active improvement of the acoustic absorption of poroelastic composites

The general idea of active improvement of the acoustic absorption of poroelastic composites can be explained as follows:

- A harmonic acoustic wave propagates in the air onto the interface between the air and a poroelastic layer (or composite). Higher frequency waves can be well absorbed by the layer but at lower frequencies the acoustic absorption of thin layers is very poor.
- Now, the acoustic wave continues to propagate in the porous medium and is reflected by the rigid wall. In fact, there are three waves: a slow longitudinal wave in the fluid phase (the so-called fluid-borne wave in the 'smeared' air of the pores), a fast longitudinal wave in the solid phase (the so-called solid-borne wave in the 'smeared' elastic skeleton) and a shear wave in the solid phase. At lower frequencies all these waves are strongly coupled so that the vibrations of elastic skeleton are coupled with the vibrations of the air in the pores.
- Because of this coupling the acoustic absorption may be actively modified by affecting the vibrations of the elastic skeleton. To this end, active implants are embedded into the porous layer and an appropriate harmonic excitation signal is applied onto the electrodes of the piezoelectric parts of the implants.

The results presented in this section show the feasibility of this approach.

Figure 6 shows the amplitudes of vibrations of the solid phase of porous foams with no implants. They are calculated for the 16 mm-thick layers of the foams subject to the harmonic excitation by the acoustic pressure of amplitude $p_0 = 2\sqrt{2}\,\mathrm{Pa}$, which means that the root-mean-square pressure equals $p_{\mathrm{rms}} = 2\,\mathrm{Pa}$ and that gives the sound pressure level of 100 dB (with the reference pressure $p_{\mathrm{ref}} = 2 \times 10^{-5}\,\mathrm{Pa}$). These amplitudes indicate the order of maximal displacements of the elastic skeleton. Two curves are plotted for each foam:

- the amplitude of vibrations at the free interface (between the layer and the air), that is at $x_1 = 16\,\mathrm{mm}$,
- the maximal amplitude for $x_1 \in [0\,\mathrm{mm}, 16\,\mathrm{mm}]$, that is for the whole domain of the layer.

It can be noticed that for lower frequencies, respectively under 3100 Hz (foam A) or 2300 Hz (foam B), the both curves are the same since the maximal amplitudes of layer vibrations are at the free interface. An important observation is that for the pressure level of 100 dB the maximal amplitudes of vibrations of the

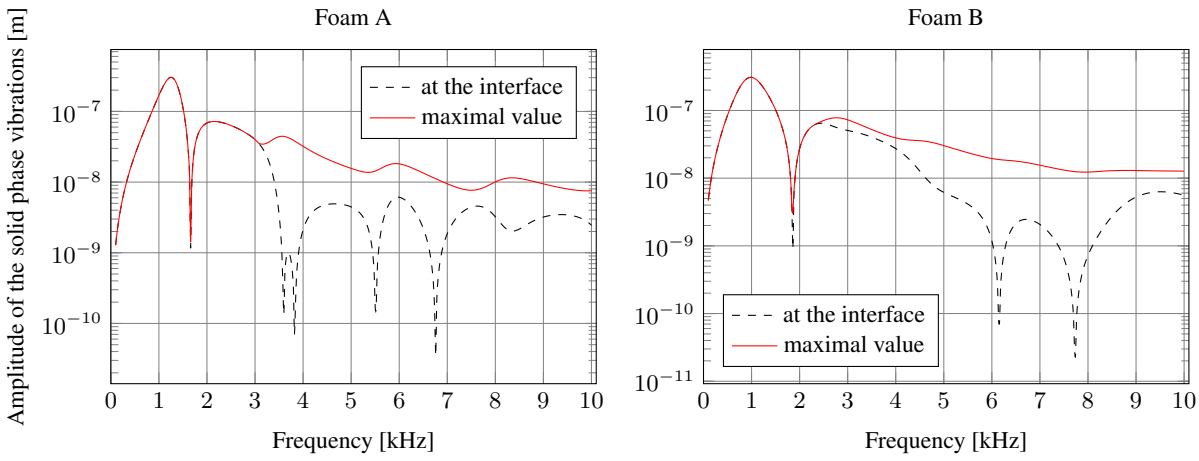


Figure 6: The amplitudes of vibrations of the solid phase (elastic skeleton) of the 16 mm-thick porous layers subject to the harmonic pressure excitation with the amplitude $p_0 = 2\sqrt{2}\,\mathrm{Pa}$

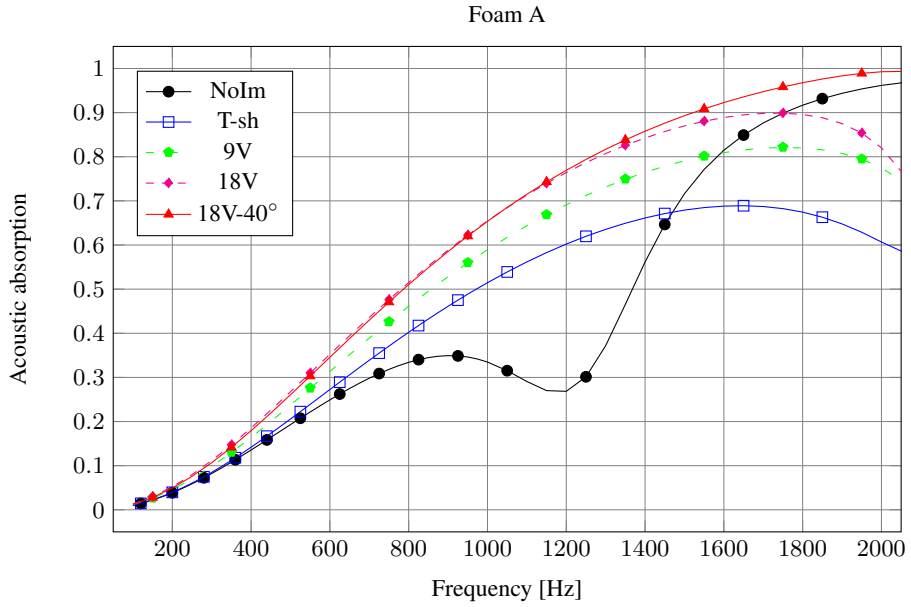


Figure 7: Active and passive absorption curves for the porous composite/layer made of the foam A

elastic skeletons of both porous layers slightly exceed $3 \times 10^{-7}$ m. The order of magnitude of the amplitudes of vibrations of the fluid phase is bigger. One should be reminded, however, that the vibrations of elastic skeleton are strongly coupled (at lower frequencies) with the vibrations of the air in the pores. To investigate the potential of this interaction is an important purpose of this paper.

As explained previously the fixed parts of the T-shaped implants can be active – they are thin patches of piezoelectric ceramic PZT4, through-thickness polarized, 9 mm long and 0.34 mm thick (see Figure 3). It was checked that by applying a voltage onto their electrodes these piezo-patches would stretch almost $10^{-8}$ m/V, which means that, for example, a signal with the amplitude of 20 V would extend the active implant for nearly $2 \times 10^{-7}$ m. Notice that this amplitude is of the same order of magnitude as the maximal amplitude of vibrations of the elastic skeleton of the considered porous layer subject to a harmonic noise of 100 dB. Thus, the active implants may affect the vibrations of elastic skeleton in order to improve the acoustic absorption of the active poroelastic composite. The results presented below prove the feasibility of this assumption.

Figure 7 shows passive and active absorption curves of the porous layer/composite made of the foam A in the frequency range from 100 to 2000 Hz. As mentioned above, for the active absorption a harmonic excitation signal is applied onto the electrodes of the piezoelectric parts of the T-shaped implants. The frequency of the signal equals to the frequency of the acoustic wave, and for the considered range the same constant voltage amplitude $\Delta\hat{V}^{\mathrm{pz}}$ is assumed. Three cases are presented which differ by the value of the amplitude and phase of signals (the phase angle of $0^\circ$ means the maximal extension of the implant):

- $\Delta\hat{V}^{\mathrm{pz}} = 9$ V, no phase shift,
- $\Delta\hat{V}^{\mathrm{pz}} = 18$ V, no phase shift,
- $\Delta\hat{V}^{\mathrm{pz}} = 18$ V with the phase of $40^\circ$.

In general, in the considered range under 2100 Hz all signals improve the acoustic absorption of the composite, however, only the one with the phase shift gives always better absorption than the layer without implants. Moreover, this phase shift must be changed in the range of 2100-2500 Hz to maintain this effect (above 2500 Hz no active approach is necessary). Notice that the absorption is significantly improved especially between 700 and 1500 Hz. For example, for the frequency 1200 Hz the acoustic absorption of the porous composite in the active state is 0.77 which is 28% better than the absorption 0.60 of this composite in the

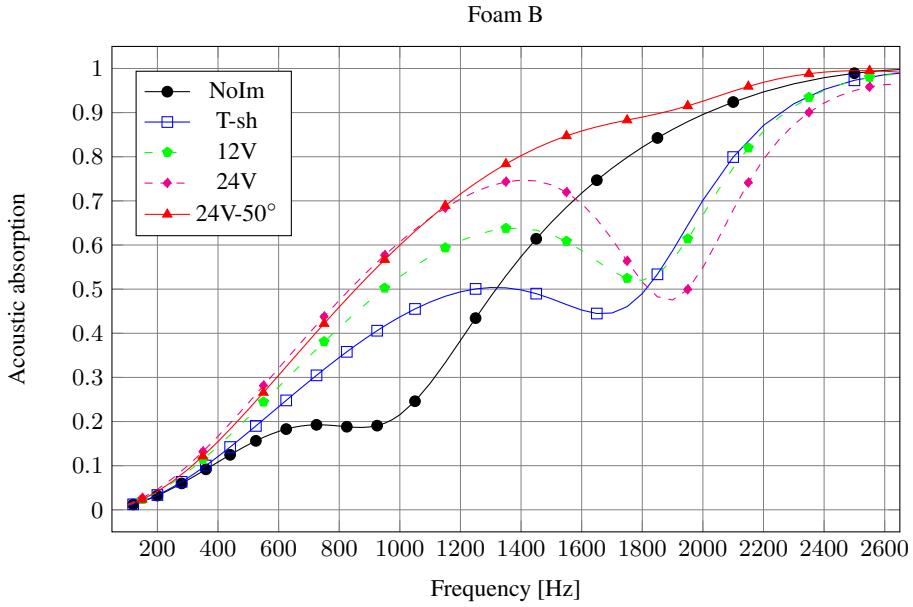


Figure 8: Active and passive absorption curves for the porous composite/layer made of the foam B

passive state and 185% better than the absorption 0.27 of the simple porous layer; the improvement between the porous layer and the passive composite is 122%. For lower frequencies the improvement is very weak, and for very low frequencies the absorption is very poor which is obvious when one remembers that the porous layer has only 16 mm. Another interesting observation is that the phase shift effect tends to be visible only when the frequency increases.

Figure 8 presents passive and active absorption curves for the composite made of the foam B. The frequency range reaches 2600 Hz – above this frequency the passive absorption of the layer with implants is very good (from 0.8 to 1.0) and it is almost identical with the absorption of the "homogeneous" layer (see the lower graph in Figure 5). Here, the results of active approach are presented for:

- $\Delta\hat{V}^{\mathrm{pz}} = 12\,\mathrm{V}$, no phase shift,
- $\Delta\hat{V}^{\mathrm{pz}} = 24\,\mathrm{V}$, no phase shift,
- $\Delta\hat{V}^{\mathrm{pz}} = 24\,\mathrm{V}$ with the phase of $50°$,

where $\Delta\hat{V}^{\mathrm{pz}}$ is the voltage amplitude of the signal; it is assumed constant in the considered frequency range, and the phase angle of $0°$ means the maximal extension of the implant. As it can be seen from Figure 8 the last signal gives the best performance of the acoustic absorption in the whole range from 100 to 2600 Hz. Confirmed is the observation that the phase shift (of $50°$) has almost no effect below some frequency (1200 Hz in this case); however, it plays an important role above this frequency.

## 7 Conclusions

Thin layers of porous foams with active and passive implants were modeled and analyzed in order to asses their acoustic absorption. The porous foams were modeled using the advanced biphasic Biot's theory of poroelasticity because the elastic vibrations of the skeleton of the foams cannot be neglected and actually play an important role in the problem. The obtained results allow to draw the following general conclusions:

- The proposed T-shaped implants (in the passive state) improve the acoustic absorption of a thin porous layer in some range of lower frequencies (where the absorption is poor), but can decrease it in another

range of higher frequencies (where altogether, the absorption is better). Similar statement is also valid for stripes of aluminium foil embedded inside the porous layer. For the lowest frequencies and above some high frequency there is no difference in the absorption curves of the porous layer with or without implants.

- The actuators in the form of thin patches of PZT ceramic are able to extend enough to affect the vibrations of the elastic skeleton of polyurethane foams induced by acoustic waves. This influence is better for the proposed T-shaped implants.
- At lower frequencies the coupling between the solid-borne waves (of the elastic skeleton) and the fluid-borne wave (of the air in the pores) is strong enough to allow the exploitation for the improvement of acoustic absorption by the proposed active approach.
- Electric signals with the amplitudes of the order of magnitude of 10 or 20 V, applied to the active piezoelectric parts of the implants, give significant improvement of the acoustic absorption of porus composites subject to the acoustic pressure excitation of 100 dB. A phase shift in the signal is necessary to achieve this improvement in the whole frequency range of interest, although it is important only above some frequency (below its effect is insignificant).

## Acknowledgements

The author would like to acknowledge the financial support from the projects 3T11F00930 and SHMCS R0301502 granted by the State Committee for Scientific Research in Poland.

## References

[1] M. R. F. Kidner, C. R. Fuller, and B. Gardner. Increase in transmission loss of single panels by addition of mass inclusions to a poro-elastic layer: Experimental investigation. *J. Sound Vib.*, 294:466–472, 2006.

[2] F.-C. Lee and W.-H. Chen. On the acoustic absorption of multi-layer absorbers with different inner structures. *J. Sound Vib.*, 259(4):761–777, 2003.

[3] M. A. Biot. The theory of propagation of elastic waves in a fluid-saturated porous solid. *J. Acoust. Soc. Am.*, 28:168–191, 1956.

[4] J. F. Allard. *Propagation of Sound in Porous Media. Modelling Sound Absorbing Materials*. Elsevier, 1993.

[5] N. Atalla, R. Panneton, and P. Debergue. A mixed displacement-pressure formulation for poroelastic materials. *J. Acoust. Soc. Am.*, 104(3):1444–1452, September 1998.

[6] P. Debergue, R. Panneton, and N. Atalla. Boundary conditions for the weak formulation of the mixed (u,p) poroelasticity problem. *J. Acoust. Soc. Am.*, 106(5):2383–2390, November 1999.

[7] N. Atalla, M. A. Hamdi, and R. Panneton. Enhanced weak integral formulation for the mixed (u,p) poroelastic equations. *J. Acoust. Soc. Am.*, 109(6):3065–3068, June 2001.